



# NANOCARBON PRODUCTS OBTAINED FROM SECONDARY RAW MATERIALS FOR MODIFICATION OF COMPOSITION COATINGS

T. Marsagishvili,<sup>[a]</sup> G. Tatishvili,<sup>[a]</sup> N. Ananiashvili,<sup>[a]</sup> J. Metreveli,<sup>[a]</sup> M. Gachechiladze,<sup>[a]</sup> E. Tskhakaia,<sup>[a]</sup> M. Machavariani,<sup>[a]</sup> N. Giorgadze,<sup>[a]</sup> and Z. Samkharadze<sup>[a]</sup>

**KEYWORDS:** nanocarbon, composition coating, tribological properties, electrodeposition, friction coefficient, secondary raw material

We obtained carbon composite materials with desired mechanical characteristics, electrical conductivity, magnetic properties, which are widely used in the production of rubbers, cables, sorption materials from various secondary raw materials like wastes of agricultural production (sawdust, fruit bones, coal industry wastes, etc.) with using a new thermochemical method. The composition of the obtained materials was carried out with scanning electron microscopy (SEM); Surface and porosity of the obtained materials were measured by use of instrument Gemini VII. Electrochemical Cu–C coatings were obtained with the use of carbon nanomaterials and tribological properties of the obtained coatings were investigated. The nanocarbon particles with large specific surface area and high porosity could also be used in composition electrocoating (CEC). The optimal concentration of carbon nanomaterials when CECs have best tribological properties has been determined.

\*Corresponding Author's

E-Mail: tati@iice.ge; tatigia@yahoo.com

[a] R. Agladze Institute of Inorganic Chemistry and Electrochemistry of the Javakishvili Tbilisi State University; 11, Mindeli str., Tbilisi, 0186, Georgia

## INTRODUCTION

The advanced level of fundamental research of condensed systems has led to a unique opportunity to create new devices and equipment. Today, small devices that consume low energy and at the same time perform the functions of a complex of devices are becoming increasingly popular. To create such devices, new often nano-sized particles play a significant role. The interaction of nanoscale particles with a solid matrix into which these particles are introduced depends on the properties, size and distribution of nanoparticles. Using these materials, we can obtain composite materials with desired mechanical characteristics, electrical conductivity, magnetic properties and likes.

At the same time, the utilization of devices, equipment and materials that are unsuitable for further operation becomes urgent. The ability to extract components useful for further use from them often makes it possible to reduce using and production of new materials significantly.

One of the tasks of the present work is to obtain nanocarbon materials, which are very widely used in the production of rubbers, cables, sorption materials, etc. Appropriately, the waste of the agricultural output containing carbon is also of interest.

In this connection, nanocarbon particles, because of their large specific surface area and high porosity, as subminiature structures may be used in composition

electrocoating (CEC). In order to modify the surface of metal products and impart them new properties, composition electrocoatings are the most suitable materials.

The process of CEC (electric composition coatings) formation is influenced by many factors,<sup>1,2</sup> one among them is the nature of the material used for the modification. It is possible to create modified, composite metal coatings of multifunctional purpose with unique properties by using this type of nanocarbon materials.<sup>3</sup> In conventional coarse-grained coatings these properties cannot be achieved. □

The other task of the present work is the creation of CEC on the basis of copper plus nanocarbon, with improved tribological properties and study of the kinetics of the electrodeposition process in the presence of the carbon phase. □

## EXPERIMENTAL

The measurements were carried out on devices: Hitachi TM 3030 Plus – Scanning electron microscope (SEM) for determination of the composition of the materials (K-series), (Figures 1 and 2; Tables 1, 2, 3) and Gemini VII for determination of surface area and porosity (Table 4).

The coating studies were carried out using the standard copper coating electrolyte of the following composition, g L<sup>-1</sup>: CuSO<sub>4</sub>·5H<sub>2</sub>O – 200 and H<sub>2</sub>SO<sub>4</sub> – 50 at pH = 0.35, with constant stirring with a magnetic stirrer. The concentration of carbon nanoparticles in the electrolyte was from 1.0 to 25.0 g L<sup>-1</sup>. For better wetting and uniform distribution of the dispersed nanomaterial, the carbon particles were treated with ethyl alcohol, filtered, and thoroughly mixed with the electrolyte. Coatings were applied to the steel plates and the ends of the bushings with an area of 3 cm<sup>2</sup>. The copper plate served as the anode. The thickness of the coatings was

approximately  $\sim 25\text{--}40\ \mu\text{m}$ . The morphology of the surface of copper coatings was studied using a Euromex microscope.

Tribotechnical tests were carried out on an inertial friction test machine by a particular method at a load of 0.1 MPa, sliding speed  $0.25\ \text{m s}^{-1}$  and at ambient temperature. The material of the counter body was steel 40 $\times$ , hardness 60HRC. Running-in was carried out at this same load until the complete contact was established over the entire friction surface. The coefficient of friction was determined for the steady-state friction regime without lubrication.

## RESULTS AND DISCUSSION

Tables 1–3 contain data obtained by the SEM measurements for the composition of the samples of sawdust, nectarine kernel and activated coal (particle size  $40\ \mu\text{m}$ ). The surface and spectra of a sawdust sample studied by SEM, with magnification 40 $\times$  can be seen on Fig.1 and 2 respectively.

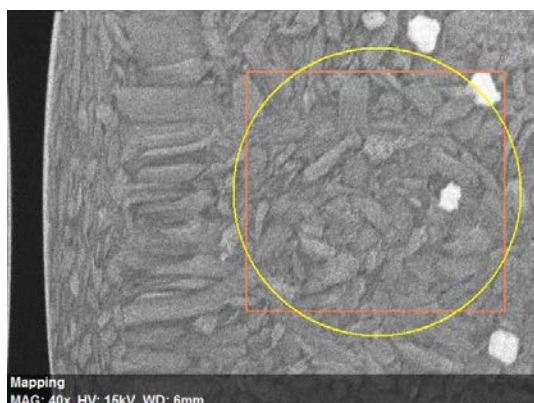


**Figure 1.** Micrograph of the surface of sawdust sample studied on SEM, with magnification 40 $\times$ .

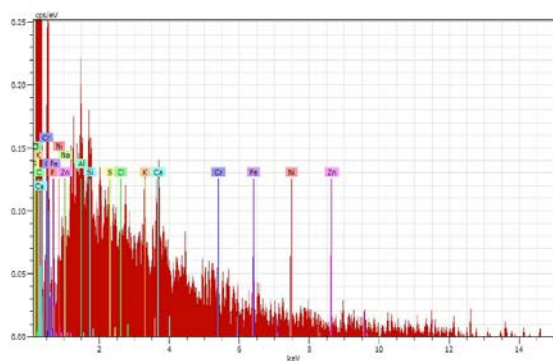


**Figure 2.** Spectra of sawdust sample studied on SEM.

The amount of zinc, sulfur, and chlorine in the sawdust based product, the amount of zinc, silicon, copper, nitrogen and chromium in the nectarine kernel based product, and the amount of chromium, lead and nitrogen in the activated carbon samples, while the amount of sodium and nickel in all, three products were below the detection limit.

To study the effect of carbon nanomaterial on copper electrodeposition, optimal conditions for obtaining CEP Cu–C were determined.

**Table 1.** EDAX composition of sawdust sample.

Element	Atomic number	Carbon content, %	
		weight	atom
Carbon	6	91.27	93.74
Oxygen	8	7.65	5.90
Calcium	20	0.41	0.13
Potassium	19	0.21	0.07
Iron	26	0.15	0.03
Chromium	24	0.10	0.02
Aluminum $\square$	13	0.08	0.04
Silicon	14	0.07	0.03
Fluorine	9	0.06	0.04

**Table 2.** EDAX composition of nectarine kernel sample.

Element	Atomic number	Carbon content, %	
		weight	atom
Carbon	6	92.36	94.53
Oxygen	8	6.71	5.15
Iron	26	0.28	0.06
Aluminum $\square$	13	0.23	0.10
Potassium	19	0.16	0.05
Chromium	24	0.10	0.02
Calcium	20	0.15	0.04
Sulfur	16	0.07	0.03
Fluorine	9	0.03	0.02

**Table 3.** EDAX composition of activated carbon sample.

Element	Atomic number	Carbon content, %	
		weight	atom
Carbon	6	89.05	92.26
Oxygen	8	9.10	7.08
Calcium	20	0.77	0.24
Zinc	30	0.30	0.06
Fluorine	9	0.06	0.04
Potassium	19	0.21	0.07
Aluminum $\square$	13	0.15	0.07
Silicon	14	0.08	0.03
Sulfur	16	0.07	0.03
Iron	26	0.03	0.01

**Table 4.** BET surface area,  $t$ -plot micropores area and  $t$ -plot external surface area of samples,  $\text{m}^2\ \text{g}^{-1}$

Starting material	BET	Micropores	Outer surface $\square$
Sawdust	470.6377	369.8977	100.7400
Nectarine kernel	520.948	434.6722	86.2759
Activated carbon	828.6867	528.3176	300.3691

The current yield ( $W$ ) of copper was studied and was established for the following values of cathode current densities  $i_c$ : 0.5, 1.0, 1.5, 2.0, and 3.0 mA cm<sup>-2</sup>. The experimental data are presented in Figure 3.

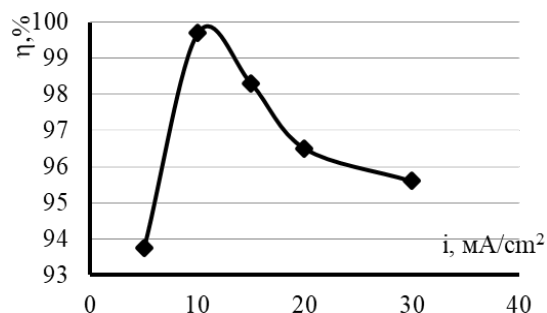


**Figure 3.** Dependence of copper current output on current density at the content in the electrolyte of carbon nanomaterial 1 g L<sup>-1</sup>.

Figure 3 shows that with a current density of 10.0 mA cm<sup>-2</sup> the current output is maximal (~100.0 %). Qualitative coatings, uniform in color and without dendrites are formed. At current densities below and above 10.0 mA cm<sup>-2</sup>, the current output of copper goes down. Further studies of the formation of CEC from this electrolyte were carried out at a current density of 10.0 mA cm<sup>-2</sup>.

The surface of a copper coating (Figure 4a) comparing to a CEC Cu-C (Figure 4b) changes and the surface of the composite coating became more grained due to the insertion of carbon nanoparticles into CEC.

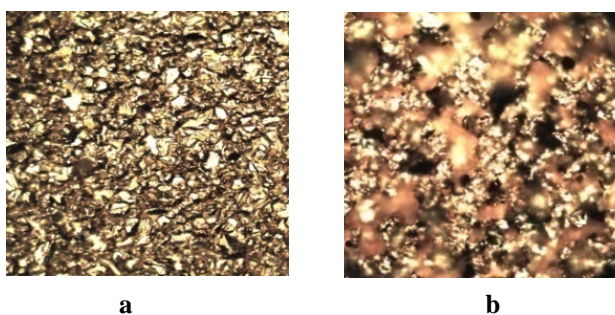


**Figure 4.** The microstructure of the surface of electrolytic copper (a) and CEC Cu-C (b). Current density  $i = 10.0$  mA cm<sup>-2</sup>.

The inclusion of carbon nanomaterial into the coating leads to structural changes in the metal matrix, which affects the exploitation properties of the electrolytic deposit. The best tribological properties characterized by a coefficient of sliding friction ( $f$ ) was available at 15 g L<sup>-1</sup> carbon concentration. (Table 4). As can be seen from Table 4, the values of the friction coefficient  $f$  for Cu-C deposits are three times lower compared to the copper deposit, and a 12-fold decrease in the wear. This is the consequence of the lubrication effect of the dispersed carbon nanomaterial in the copper coatings.

**Table 4.** Tribological properties of copper coatings at the concentration of dispersed phase of 15.0g/l.

Material	Friction			Wear, mg h <sup>-1</sup>
	Rate $v$ , m/s	Temp., °C	Sliding coefficient	
Copper	0.125	55	1.0	102
Cu-C (steel 45 substrate)	0.125	32	0.32	8
Cu-C (stainless steel substrate)	0.125	28	0.29	6

## CONCLUSIONS

Nanocarbon materials from various secondary raw materials (sawdust, fruit bones, coal industry wastes, etc.) were obtained by the thermochemical method. The tribological properties of the Cu-C electrochemical coatings obtained with the use of carbon nanomaterials were investigated. The best tribological properties of Cu-C CEC were obtained at 15 g L<sup>-1</sup> carbon content used during the electrolysis. The values of the friction coefficient  $f$  decreased by three times in comparison to copper deposit, with a 12-fold decrease in wear. This is due to the lubricating effect of carbon nanomaterial, which is included in the structure of copper coatings and performs as dry solid lubricants.

## Acknowledgment

Paper was presented at the 5th International Conference "Nanotechnologies", November 19–22, 2018, Tbilisi, Georgia (Nano-2018).

## REFERENCES

- Saifulin, R. S., *Inorganic Composition Materials*. Khimiya, Moscow, **1983**, 304; Tarasevich, M. P., *Electrochemistry of Carbonaceous Materials*. Nauka, Moscow, **1984**.
- Mingazova, G. G., Fomina, R. E., Vodopianova, S. V. and Saifulin, R.S., *Bull. KSTU*, **2012**, 20(2), 81-84.
- Arai, S., Kirihata, K., Shimizu, M., Ueda, M., Katada, A., Uejima, M., Fabrication of Copper/Single-Walled Carbon Nanotube Composites by Electrodeposition Using Free-Standing Nanotube Film, *Journal of Electrochemical Society*, 2017, 164(13), D922-D929. doi: 10.1149/2.0041714jes
- Arai, S., Osaki, T., Fabrication of Copper/Multiwalled Carbon Nanotube Composites Containing Different Sized Nanotubes by Electroless Deposition, *J. Electrochem. Soc.*, **2015**, 162(1), D68-D73. DOI:10.1149/2.0971501jes.
- Feng, Y., McGuire, G. E., Shenderova, O. A., Ke, H., Burkett, S. I., Fabrication of copper/carbon nanotube composite thin films by periodic pulse reverse electroplating using nanodiamond as a dispersing agent, *Thin Solid Films*, 2016, 615, 116-121. doi.org/10.1016/j.tsf.2016.07.015

Received: 06.01.2019.

Accepted: 18.02.2019.



# SILTY CLAY-CONTAINING SOIL CATALYZED MICROWAVE ASSISTED MULTICOMPONENT SYNTHESIS OF OCTAHYDROQUINAZOLINONE DERIVATIVES

S. S. Chine,<sup>[a]</sup> C. S. Patil<sup>[b]\*</sup> and R. P. Pawar<sup>[b]</sup>

**Keywords:** Octahydroquinazolinones; microwave-assisted synthesis; multicomponent synthesis; heterogeneous silt catalyst.

An efficient protocol was developed for the synthesis of octahydroquinazolinone derivatives in presence of silty clay-containing soil in solvent free conditions under microwave irradiation. The isolated products were characterized by FTIR, <sup>1</sup>HNMR and <sup>13</sup>C NMR spectroscopy. The catalyst was characterized by wet chemical analysis, SEM, EDS, XRD and IR spectroscopy.

\*Corresponding Authors

Fax: +9102402334430

E-Mail: [patil.sheelal1962@gmail.com](mailto:patil.sheelal1962@gmail.com),

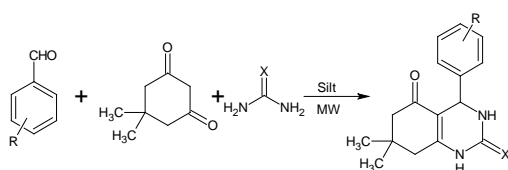
[sonalichine85@gmail.com](mailto:sonalichine85@gmail.com)

[a] Department of Engineering Sciences, SRES Sanjivani College of Engineering (S.P.P.U, Pune), Kopergaon, Dist. Ahmednagar, 423601, (M.S.), India.

[b] Department of Chemistry, Deogiri College Aurangabad, 431005, (M.S.), India.

## Introduction

Octahydroquinazolinone derivatives is an important class of organic compounds because of their pharmacological activities such as antihypertensive,<sup>1</sup> antibacterial,<sup>2,3</sup> antitumor,<sup>4</sup> anti-inflammatory etc.<sup>5</sup> Multicomponent reactions (MCRs) have apparently been a route to the synthesis of large number of complex molecules from readily available building blocks.<sup>6</sup> Octahydroquinazolinones synthesis is a modified Biginelli reaction.<sup>1</sup> Octahydroquinazolinone have been synthesized using aromatic aldehydes, dimedone and urea/thiourea in presence of various catalysts such as montmorillonite,<sup>7</sup> zeolites,<sup>8</sup> boron compounds,<sup>9</sup> Zn(OTf)<sub>2</sub>,<sup>3</sup> conc. H<sub>2</sub>SO<sub>4</sub>,<sup>10</sup> ionic liquids,<sup>11</sup> ion exchange resins,<sup>12</sup> Trimethyl silyl chloride,<sup>13</sup> Nafion-H,<sup>14</sup> VOSO<sub>4</sub>,<sup>15</sup> conc. HCl,<sup>16</sup> Fe(NO<sub>3</sub>)<sub>3</sub>·9H<sub>2</sub>O,<sup>17</sup> silica sulfuric acid,<sup>18</sup> t-BuOK,<sup>19</sup> TiO<sub>2</sub>,<sup>20</sup> ammonium metavanadate,<sup>21</sup> Cu(OTf)<sub>2</sub>,<sup>22</sup> phosphotungstic acid nanoclusters,<sup>23</sup> BMI.InCl<sub>4</sub>,<sup>24</sup> SiO<sub>2</sub>-NaHSO<sub>4</sub>,<sup>25</sup> ZnO<sub>2</sub> nanoparticles,<sup>26</sup> phytic acid,<sup>27</sup> lanthanum oxide,<sup>28</sup> Naion-Ga,<sup>29</sup> CuS QDs,<sup>30</sup> ZrOCl<sub>2</sub>·8H<sub>2</sub>O,<sup>31</sup> Cu/SiO<sub>2</sub>,<sup>32</sup> β-cyclodextrin, aqueous hydrotropic solution of Na-p-Toluene sulfonic acid under microwave irradiation (MW),<sup>33</sup> BF<sub>3</sub>·SiO<sub>2</sub>,<sup>34</sup> Aluminate Sulfonic Acid Nanoparticles,<sup>35</sup> Ion exchange resin Nafion<sup>12</sup> H<sub>4</sub>CuPW<sub>11</sub>O<sub>39</sub>,<sup>36</sup> polyvinyl polyvinylpolypyrrolidine supported chlorosulfonic acid,<sup>37</sup> and molybdenum based heterogeneous catalysts (MoO<sub>2</sub>(acac)<sub>2</sub> on zeolite)<sup>38</sup> under MW irradiation.<sup>39</sup>



**Scheme 1.** Synthesis of Octahydroquinazolinones using silt catalyst

## Experimental

All the chemicals used without further purification and were of AR grade. Microwave irradiation was done in RAGA'S Scientific Microwave system. Synthesized products were characterized by IR, <sup>1</sup>HNMR and <sup>13</sup>C NMR spectroscopy data and melting points. Melting points were recorded in an open capillary and were uncorrected. IR spectra were recorded using Perkin-Elmer spectrometer with ATR technology. <sup>1</sup>HNMR and <sup>13</sup>C NMR spectra were recorded on 500MHz Bruker FT-NMR spectrometer using CDCl<sub>3</sub> solvent.

### Catalyst preparation

The silty soil collected from bed of Godavari River, Kopergaon, A.Nagar, India. The silt is naturally available granular brown colour material having particle size (0.05-0.002mm), it may occur as soil. Chemical composition of collected silty soil was calculated by wet chemical analysis method reported in Table 1.

**Table 1.** Silty soil composition by wet chemical analysis

Constituent	Silty clay-containing soil %
sand	41.93
clay	19.35
silt	38.70

### Activation of silt

Received silty clay-containing soil was sieved through different mesh sizes to remove any coarse material and to get uniform particle. This silty clay containing soil was kept at temperature of 400°C in silica crucible for 1h in an electric oven for activation and used as silty clay-containing soil catalyst for investigation. The average diameter of silty clay-containing soil used is about 50 μm (Figure 1)

### General procedure for the synthesis of octahydroquinazolinones under MW

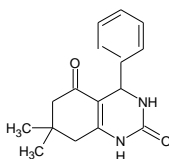
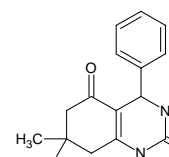
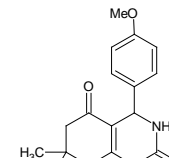
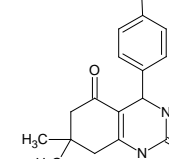
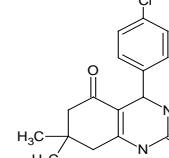
Synthesis of octahydroquinazolinones were done using a mixture of aromatic aldehyde (1.0 mmol), dimedone (1.0

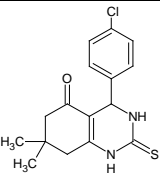
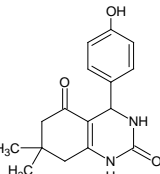
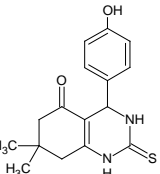
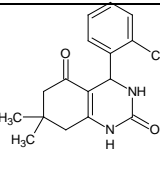
**Table 2.** Optimization of reaction conditions from 4-chlorobenzaldehyde, dimedone and urea

Entry	Catalyst / Solvent	Condition	Reaction time, min	<sup>a</sup> Yield, %
1	Nocatalyst/CHCl <sub>3</sub>	R.T	180	NoReaction
2	Nocatalyst/CHCl <sub>3</sub>	Reflux	180	22
3	Catalyst (20 wt%)/CHCl <sub>3</sub>	Reflux	60	62
4	Catalyst (20 wt%)/EtOH	Reflux	60	73
5	Nocatalyst/---	MW 240 W	35	36
6	Nocatalyst/---	MW 300 W	30	48
7	Catalyst (20 wt%)/EtOH	MW 300 W	20	82
8	Catalyst (20 wt%)/---	MW 240 W	20	80
9	Catalyst (10 wt%)/---	MW 300 W	20	78
10	Catalyst (20 wt%)/---	MW 300 W	20	94

**ReactionCondition:** 4-chlorobenzaldehyde (1.0 mmol), dimedone (1.0 mmol), urea (1.2 mmol) and silty-soilcatalyst

**Table 3.** Synthesis of octahydroquinazolinone catalyzed by silty clay-containing soil from benzaldehydes, urea (thiourea) and dimedone

Entry	R in RC <sub>6</sub> H <sub>4</sub> CHO	X in (H <sub>2</sub> N) <sub>2</sub> C=X	Product	Reaction time, min	Yield, % <sup>[a]</sup>	M.P.	
						Found	Literature
4a	H	O		10	96	96	291
4b	H	S		15	86	218	218-219
4c	4-MeO	O		15	89	246	246-247
4d	4-MeO	S		20	80	275	273-275
4e	p-Cl	O		20	94	301	304-306

<b>4f</b>	p-Cl	S		15	87	290	288-290
<b>4g</b>	p-OH	O		15	90	301	300-302
<b>4h</b>	p-OH	S		20	86	280	--
<b>4i</b>	o-Cl	O		15	89	284	282-285

mmol) and urea/thiourea (1.5 mmol) and silt (20 wt %) taken in round bottom flask and kept in MW at 300 W for required time (Table 3). The progress of reaction was monitored by thin layer chromatography using ethyl acetate: hexane solvent system. On completion of reaction, the reaction mass was filtered and concentrated. Isolation of catalyst and purification of product was done by recrystallisation using ethanol (Scheme1).Results and discussion

Catalyst has been characterized using XRD, FTIR, SEM and EDS, techniques.

#### X-ray diffraction analysis

To determine various minerals present in silt soil, X-ray diffraction study was carried out on Philips, Holland X-ray diffractometer. The XRD of the silty clay-containing soil is given in the supplementary material. By correlating the results with JCPDS database, silt consists of components having SiO<sub>2</sub>, Al<sub>2</sub>O<sub>3</sub>, Fe<sub>2</sub>O<sub>3</sub>, TiO<sub>2</sub>, potassium, sodium, magnesium and calcium oxide building components (Figure 2).<sup>40-45</sup>

S. No.	Component	%
1	SiO <sub>2</sub>	38
2	Al <sub>2</sub> O <sub>3</sub>	19
3	Fe <sub>2</sub> O <sub>3</sub>	9
4	TiO <sub>2</sub>	5
5	K <sub>2</sub> O	2
6	Na <sub>2</sub> O	3
7	CaO	1

#### SEM and EDS analysis

The study of morphology and elemental composition was carried out by Scanning Electron Microscopy and Energy Dispersive Spectroscopy. The electron microphotographs were recorded on JEOL-JSM-6360A operating at 20KV. The catalyst sample is analyzed under SEM at different magnification. Figure 3 shows silty clay containing soil morphologies which contains oxygen, Na, Mg, Al, Si, Cl, K, Ca, Ti, Fe. The scanning electron microphotograph of silt shows the particle size to be around 50µm. The typical aggregate structure of material has been observed.

#### Infrared spectroscopy (FT-IR)

FT-IR study of catalyst was done to confirm presence of silica, iron and aluminum. The distinct band at 3612.7cm<sup>-1</sup> and 3621cm<sup>-1</sup> indicate existence of isolated OH group of Si and Al. The band at 462.02 cm<sup>-1</sup> indicates O-Si-O bending mode whereas band at 1185.80 cm<sup>-1</sup>, 992.06 cm<sup>-1</sup>, 797.45 cm<sup>-1</sup> signify occurrence of Si-O-Fe, Al-OH and Fe-OH vibrations, respectively. The bands at 536.84 cm<sup>-1</sup>, and 451.85 cm<sup>-1</sup> are due to Fe-O bond stretching.

#### Optimization of reaction conditions

Optimization of reaction conditions were done on model reaction of benzaldehyde (1mmol), dimedone (1mmol) and urea (1.2mmol), with silt catalyst under microwave irradiation. It is represented in Table 2.The generability of this method was studied by performing the reaction of several substituted aromatic aldehyde, dimedone and

urea/thiourea using silt as a catalyst under MWI without solvent. The results are summarized in Table 3.

### Spectral data

**4a: 4-Phenyl-7,7-dimethyl-1,2,3,4,5,6,7,8-octahydroquinazoline-2,5-dione**, M.p.: 291 °C, FT-IR (cm<sup>-1</sup>): 3380, 3260, 3130, 2940, 1697, 1620, 1455, <sup>1</sup>H NMR (500 MHz, DMSO-d<sub>6</sub>, TMS, ppm): 0.89 (s, 3H, -CH<sub>3</sub>), 1.02 (s, 3H, -CH<sub>3</sub>), 2.01-2.04 (d, 1H, CH, J=13 Hz), 2.18-2.21 (d, 1H, CH, J=13 Hz), 2.25-2.29 (d, 1H, CH, J=13 Hz), 2.39-2.43 (d, 1H, CH, J=13 Hz), 5.15 (s, 1H, CH), 7.20-7.24 (m, 3H, ArH), 7.29-7.32 (m, 2H, ArH), 7.76 (bs, 1H, NH), 9.4 (bs, 1H, NH) <sup>13</sup>C NMR (DMSO-d<sub>6</sub>, TMS, ppm): 27.30, 29.22, 32.76, 50.28, 52.43, 107.86, 126.69, 127.59, 128.77, 145.10, 152.39, 152.85, 193.33.

**4e: 4-(4-Chlorophenyl)-7,7-dimethyl-4,6,7,8-tetrahydroquinazoline-2,5(1H,3H)-dione**, M.p.: 301 °C, FTIR (cm<sup>-1</sup>): 3320, 3242, 2960, 1705, 1670, 1613, 1488, 1418 <sup>1</sup>H NMR (TMS, ppm): 0.88 (s, 3H, -CH<sub>3</sub>), 1.01 (s, 3H, -CH<sub>3</sub>), 2.01-2.04 (d, 1H, CH, J=13 Hz), 2.17-2.21 (d, 1H, CH, J=13 Hz), 2.25-2.28 (d, 1H, CH, J=13 Hz), 2.39-2.42 (d, 1H, CH, J=13 Hz), 5.15 (s, 1H, CH), 7.24-7.25 (d, 2H, ArH, J=6.76 Hz), 7.37-7.39 (d, 2H, ArH, J=6.7 Hz), 7.80 (s, 1H, NH), 9.52 (s, 1H, NH). <sup>13</sup>C NMR (DMSO-d<sub>6</sub>, TMS, ppm): 27.31, 29.16, 32.75, 50.23, 51.94, 107.48, 128.59, 128.76, 132.07, 144.06, 152.21, 153.03, 193.35.

**4i: 4-(2-Chlorophenyl)-7,7-dimethyl-4,6,7,8-tetrahydroquinazoline-2,5(1H,3H)-dione**, M.P.: 284 °C FTIR (cm<sup>-1</sup>): 3253, 3090, 2953, 1698, 1640, 1430, 1372, <sup>1</sup>H NMR: 0.96 (s, 3H, -CH<sub>3</sub>), 1.03 (s, 3H, -CH<sub>3</sub>), 1.97-2.00 (d, 1H, CH, J=13 Hz), 2.15-2.18 (d, 1H, CH, J=13 Hz), 2.31-2.34 (d, 1H, CH, J=13 Hz), 5.56 (s, 1H, CH), 7.23-7.32 (m, 3H, ArH), 7.38-7.39 (m, 1H, ArH), 7.7 (s, 1H, NH), 9.5 (s, 1H, NH) <sup>13</sup>C NMR (DMSO-d<sub>6</sub>, TMS, ppm): 27.52, 29.19, 32.71, 50.26, 51.08, 106.29, 127.87, 129.42, 129.88, 129.99, 132.33, 141.68, 151.54, 153.50, 193.08.

### Conclusion

The most important advantage of this method is use of naturally available, economical and competent silt catalyst. It works without solvent under microwave irradiation in short time. This implicates fruitful addition to the non-conventional methods for the synthesis of octahydroquinazolinone derivatives.

### Acknowledgement

Authors are thankful to the Principal S.R.E.S', Sanjivani College of Engineering (S.P.P.U, Pune), Kopergaon and Principal Deogiri College (Dr. B.A.M.U, Aurangabad), Aurangabad for providing necessary research facilities and constant encouragement.

### References

- Biginelli, P., Synthesis of 3,4-Dihydropyrimidin-2(1H)-ones, *Gazz. Chim. Ital.*, **1893**, *23*, 360-413.
- Kidwai, M., Saxena, S., Khan, M. K. R., Thukral, S. S., Synthesis of 4-aryl-7,7-dimethyl-1,2,3,4,5,6,7,8- octahydroquinazolinone-2-one/ thione-5-one derivatives and evaluation as antibacterials, *Eur. J. Med. Chem.*, **2005**, *40*(8), 816-819. <https://doi.org/10.1016/j.ejmech.2005.02.009>
- Shah, P. M., Patel, M. P., Zn(OTf)<sub>2</sub>- catalyzed three component, one-pot cyclocondensation reaction of some new octahydroquinazolinone derivatives and access their potential, *Med. Cem. Res.*, **2012**, *21*(7), 1188-1198. <https://doi.org/10.1007/s00044-011-9628-y>
- Suresh, Sandhu J. S., Past, present and future of Biginelli reaction: a critical perspective, *Arkivoc*, **2012**, *1*, 66-133. <http://dx.doi.org/10.3998/ark.5550190.0013.103>
- Nofal, Z. M., Fahmy, H. H., Zarie, E. S., El-Eraky, W., Synthesis of new pyrimidine derivatives with evaluation of their anti-inflammatory and analgesic activities, *Acta Pol. Pharm.*, **2011**, *68*(4), 507-517.
- Lal, J., Gupta, S. K., Agarwal, D. D., Chitosan: An efficient biodegradable and recyclable green catalyst for one-pot synthesis of 3,4- dihydropyrimidinones of curcumin in aqueous media, *Catal. Commun.*, **2012**, *27*, 38-43. <https://doi.org/10.1016/j.catcom.2012.06.017>
- Bigi, F., Carloni, S., Frullanti, B., Maggi, R., Sartori, G., A revision of the Biginelli reaction under solid acid catalysis. Solvent free synthesis of Dihydropyrimidines over Montmorillonite KSF, *Tetrahedron Lett.*, **1999**, *40*, 3465-3468. [https://doi.org/10.1016/s0040-4039\(99\)00424-4](https://doi.org/10.1016/s0040-4039(99)00424-4)
- Rani, V. R., Srinivas, N., Kishan, M. R., Kulkarni, S. J., Raghavan, K. V., Zeolite- catalysed cyclocondensation reaction for the selective synthesis of 3,4- dihydropyrimidin-2(1H)- ones, *Green Chem.*, **2001**, *3*, 305-306. <https://doi.org/10.1039/b107612b>
- Dondono, A., Massi, A., Sabbatini, S., Bertolasi, V., Three-component Biginelli cyclocondensation reaction using C-Glycosylated substrates. Preparation of a collection of Dihydropyrimidinone Glycoconjugates and the synthesis of C- Glycosylated Monastrol analogues, *J. Org. Chem.*, **2002**, *67*, 6979-6994. doi. 10.1021/jo202076.
- Hassani, Z., Islami, M. R., Kalantri, M., An efficient one pot synthesis of octahydroquinazolinone derivatives using catalytic amount of H<sub>2</sub>SO<sub>4</sub> in water, *Bioorg. Med. Chem. Lett.*, **2006**, *16*, 4479-4482. doi. 10.1016/j.bmcl.2006.06.038
- Khurana, J. M., Kumar, S., Ionic liquid: an efficient and recyclable medium for the synthesis of octahydroquinazolinone and biscoumarin derivatives, *Monatsh. Chem.*, **2010**, *141*(5), 561-564. <https://doi.org/10.1007/s00706-010-0306-4>
- Joseph, J. K., Jain, S. L., Sain, B., Ion exchange resins as recyclable and heterogeneous solid acid catalysts for the Biginelli condensation: An improved protocol for the synthesis of 3,4- dihydropyrimidin-2-ones *J. Mol. Catal. A Chem.*, **2006**, *247*, 99-102. <https://doi.org/10.1016/j.molcata.2005.11.028>
- Kantevari, S., Bantu, R., Nagarapu, L., TMSCl mediated highly efficient one pot synthesis of octahydroquinazolinone and 1,8- dioxo-octahydroxanthene derivatives, *ARKIVOC Part(xvi).*, **2006**, 136-148. <http://dx.doi.org/10.3998/ark.5550190.0007.g15>
- Lin, H., Zhao, Q., Xu, B., Wang, X., Nafion- H catalyzed cyclocondensation reaction for the synthesis of dihydroquinazolinone derivatives, *J. Mol. Catal. A Chem.*, **2007**, *268*, 221-226. <https://doi.org/10.1016/j.molcata.2006.12.020>

- <sup>15</sup>Reddy, C.S., Raghu, M., Nagaraj, A., VOSO<sub>4</sub> catalyzed Biginelli condensation: An efficient synthesis of dihydro-1H-pyrimidine-2-thione/one and octahydro-2,5-quinazolinone, *Indian J. Chem. B*, **2009**, *48*, 1178–1182.
- <sup>16</sup>Ladani, N.K., Patel, M.P., Patel, R.G., An efficient three component one-pot synthesis of some new octahydroquinazolinone derivatives and investigation of their antimicrobial activities, *ARKIVOC VII*, **2009**, 292–302.
- <sup>17</sup>Phukan, M., Kalita, M.K., Borah, R., A new protocol for Biginelli (or like) reaction under solvent-free grinding method using Fe(NO<sub>3</sub>)<sub>3</sub>·9H<sub>2</sub>O as catalyst, *Green Chem. Lett. Rev.*, **2010**, *3*, 329-334. <https://doi.org/10.1080/17518253.2010.487841>
- <sup>18</sup>Mobinikhaledi, A., Foroughifar, N., Khodaei, H., Synthesis of octahydroquinazolinone derivatives using silica sulphuric acid as an efficient catalyst, *Eur. J. Chem.*, **2010**, *1*, 291-293. <https://doi.org/10.5155/eurjchem.1.4.291-293.108>
- <sup>19</sup>Shen, Z.-L., Xu, X.-P., Ji, S.-J., Bronsted-base catalyzed one pot three component Biginelli type reaction: An efficient synthesis of 4,5,6- Triaryl- 3,4- dihydropyrimidin- 2(1H)-one and mechanistic study, *J. Org. Chem.*, **2010**, *75*, 1162-1167. <https://doi.org/10.1021/jo902394y>
- <sup>20</sup>Kassaei, M. Z., Masroufi, H., Movahedi, F., Mohammadi, R., TiO<sub>2</sub> as a reusable catalyst for the one pot synthesis of 3,4-dihydropyrimidin- 2(1H)- ones under solvent free conditions, *Helv. Chim. Acta*, **2010**, *93*(2), 261-264. <https://doi.org/10.1002/hlca.200900197>
- <sup>21</sup>Niralwad, K.S., Shingate, B.B., Shingare, M.S., Microwave-assisted one pot synthesis of octahydroquinazolinone derivatives using ammonium metavanadate under solvent free condition, *Tetrahedron Lett.*, **2010**, *51*, 3616-3619. <https://doi.org/10.1016/j.tetlet.2010.04.118>
- <sup>22</sup>Pasunooti, K. K., Chai, H., Jensen, C. N., Gorityala, B. K., Wang, S., Liu, X.-W., A microwave assisted copper catalyzed three component synthesis of dihydropyrimidinones under mild conditions, *Tetrahedron Lett.*, **2011**, *52*, 80-84. <https://doi.org/10.1016/j.tetlet.2010.10.150>
- <sup>23</sup>Naik, M. A., Samantaray, S., Mishra, B. G., Phosphotungstic Acid Nanoclusters Grafted onto High Surface Area Hydrous Zirconia as Efficient Heterogeneous catalyst for synthesis of Octahydroquinazolines and β- Acetamido Ketones, *J. Cluster Sci.*, **2011**, *22*(2), 295-307. <https://doi.org/10.1007/s10876-011-0384-4>
- <sup>24</sup>Khatri, P. K., Jain, S. L., Sain, B., Ultrasound promoted oxidation of sulphides with high hydrogen peroxides under catalyst free conditions, *Ind. Eng. Chem. Res.*, **2011**, *50*, 701-704. <https://doi.org/10.1021/ie1013426>
- <sup>25</sup>Azzam, S. H. S., Siddekha, A., Nizam, A., Pasha M. A., SiO<sub>2</sub>-NaHSO<sub>4</sub> as an efficient reusable heterogeneous catalyst for the one pot three component synthesis of octahydroquinazolin-2,5-diones in water, *Chin. J. Catal.*, **2012**, *33*, 677-680. [https://doi.org/10.1016/s1872-2067\(11\)60366-5](https://doi.org/10.1016/s1872-2067(11)60366-5)
- <sup>26</sup>Sedeghi, B., Nasirian, Z., Hassanabadi, A., ZnO nanoparticles solid phase acidic catalyst for one pot synthesis of octahydroquinazolinone derivatives, *J. Chem. Res.*, **2012**, *36*(7), 391-392. <https://doi.org/10.3184/174751912x13371679868473>
- <sup>27</sup>Zhang, Q., Wang, X., Li, Z., Wu, W., Liu, J., Wu, H., Phytic acid: a biogenic organocatalyst for one pot Biginelli reactions to 3,4-dihydropyrimidin-2(1H)-ones/ thiones, *RSC Adv.*, **2014**, *4*, 19710-19715. <https://doi.org/10.1039/c4ra02084g>
- <sup>28</sup>Kuraitheerthakumaran, A., Pazhamalai, S., Manikandan, H., Gopalakrishnan, M., Rapid and efficient one pot synthesis of octahydroquinazolinone derivatives using lanthanum oxide under solvent free condition, *J. Saudi Chem. Soc.*, **2014**, *18*, 920-924. <https://doi.org/10.1016/j.jscs.2011.11.014>
- <sup>29</sup>SuryaPrakash, G.K., Lau, H., Panja, C., Bychinskaya, I., Ganesh, S. K., Zaro, B., Synthesis of dihydropyrimidinones/ Thiopyrimidinones: Nafion-Ga, an efficient green Lewis acid catalyst for the Biginelli reaction, *Catal. Lett.*, **2014**, *144*, 2012-2020. <https://doi.org/10.1007/s10562-014-1364-8>
- <sup>30</sup>Chaudhary, G. R., Bansal, P., Mehta, S. K., Recyclable CuS quantum dots as heterogenous catalyst for Biginelli reaction under solvent free conditions, *Chem. Eng. J.*, **2014**, *243*, 217-224. <https://doi.org/10.1016/j.cej.2014.01.012>
- <sup>31</sup>Karami, S., Karami, B., Khodabakhshi, S., Solvent free synthesis of novel and known octahydroquinazolines/ thiones by the use of ZrOCl<sub>2</sub>·8H<sub>2</sub>O as a highly efficient and reusable catalyst, *J. Chin. Chem. Soc.*, **2012**, *60*, 22-26. <https://doi.org/10.1002/jccs.201200145>
- <sup>32</sup>Heravi, M. M., Karimi, N., Hamidi, H., Oskooie, H., Cu/SiO<sub>2</sub> : A recyclable catalyst for the synthesis of octahydroquinazolinone, *Chin. Chem. Lett.*, **2013**, *24*(2), 143-144. <https://doi.org/10.1016/j.ccllet.2013.01.003>
- <sup>33</sup>Kamble, S. B., Kumbhar, A. S., Jadhav S. N., Salunkhe R. S., *Procedia Mater. Sci.*, Microwave assisted attractive and rapid process for synthesis of octahydroquinazolinone in aqueous hydrotropic solutions, **2014**, *6*, 1850-1856. <https://doi.org/10.1016/j.mspro.2014.07.215>
- <sup>34</sup>Akbari, A., Hosseini-Nia, A., Synthesis and insecticide activity of octahydroquinazolinone derivatives, *J. Appl. Chem. Res.*, **2015**, *9*(2), 7-14.
- <sup>35</sup>Esfahani, M., Taei, M., Aluminate sulfonic acid nanoparticles: synthesis characterization and application as a new and recyclable nanocatalyst for the Biginelli and Biginelli like condensations, *RSC Adv.*, **2015**, *5*(56), 44978-44989. <https://doi.org/10.1039/c5ra01406a>
- <sup>36</sup>Mozafari, R., Heidarizadeh, F., One pot synthesis of octahydroquinazolinone derivatives using (Me (Im)<sup>12</sup> ) H<sub>4</sub>CuPW<sub>11</sub>O<sub>39</sub> as a surfactant type catalyst, *J. Cluster Sci.*, **2016**, *27*(5), 1629-1643. <https://doi.org/10.1007/s10876-016-1023-x>
- <sup>37</sup>Cheghini, M. G., Mokhtary, M., Polyvinylpyrrolidone-Supported Chlorosulfonic Acid: An Efficient Catalyst for One-pot synthesis of Dihydropyrimidinones and Octahydroquinazolin-2,5-diones *Polycycl. Arom. Compd.*, **2016**, *37*(1), 63-72. <https://doi.org/10.1080/10406638.2015.1088046>
- <sup>38</sup>Hadigavabar, A. D., Tabatabaeian, K., Zanjanchi, M. A., & Mamaghani, M., Molybdenum anchored onto zeolite β: an efficient catalyst for the one pot synthesis of octahydroquinazolinone derivatives under solvent free conditions, *React. Kinet. Mech. Cat.*, **2018**, *124*(2), 857-871. <https://doi.org/10.1007/s11144-018-1370-8>
- <sup>39</sup>Choudhary, V. R., Tillu, V. H., Narkhede, V. S., Borate, H. B., Wakharkar, R. D., Microwave assisted solvent free synthesis of dihydropyrimidinones by Biginelli reaction over Si-MCM-41 supported FeCl<sub>3</sub> catalyst, *Catal. Commun.*, **2003**, *4*, 449-453. [https://doi.org/10.1016/s1566-7367\(03\)00111-0](https://doi.org/10.1016/s1566-7367(03)00111-0)
- <sup>40</sup>Mitra, S., Thakur, L., Rathore, V., Mondal, P., Removal of Pb(II) and Cr(VI) by laterite soil from synthetic waste water: single and bicomponent approach, *Desalination Water Treat.*, **2015**, *57*(39), 18406-18416. <https://doi.org/10.1080/19443994.2015.1088806>
- <sup>41</sup>Khataee, A., Salahpour, F., Fathinia, M., Seyyedi, B., Vahid, B., Iron rich laterite soil with mesoporous structure for the heterogeneous Fenton like degradation of an azo dye under visible light, *J. Ind. Eng. Chem.*, **2015**, *26*, 129-135. <https://doi.org/10.1016/j.jiec.2014.11.024>
- <sup>42</sup>Yahya, H., Othman, M. R., Ahmad, Z. A., Effect of Mullite formation on properties of aluminosilicate ceramic balls, *Procedia Chem.*, **2016**, *19*, 922-928. <https://doi.org/10.1016/j.proche.2016.03.136>



- <sup>43</sup>Deng, L., Xu, Q., Wu, H., Synthesis of Zeolite like material by hydrothermal and fusion methods using municipal solid waste fly ash, *Procedia Environ. Sci.*, **2016**, *31*, 662-667. <https://doi.org/10.1016/j.proenv.2016.02.122>
- <sup>44</sup>Ghanraja, S., Vinuthkumar, K. L., Raju, H. P., Ravikumar, K. S., Processing and Mechanical Properties of Hot Extruded Al(Mg)-Al<sub>2</sub>O<sub>3</sub> Composites, *Mater. Today Proc.*, **2015**, *2*, 1291-1300. <https://doi.org/10.1016/j.matpr.2015.07.045>
- <sup>45</sup>Chao, L., Zhiming, Z., Yongli, H., Zhenmin, C., Weikang, Y., Support effects on thiophene hydrodesulfurisation over Co-Mo-Ni/Al<sub>2</sub>O<sub>3</sub> and Co-Mo-Ni/TiO<sub>2</sub>-Al<sub>2</sub>O<sub>3</sub> catalysts, *Chin. J. Chem. Eng.*, **2014**, *22(4)*, 383-391. [https://doi.org/10.1016/s1004-9541\(14\)60038-0](https://doi.org/10.1016/s1004-9541(14)60038-0)

Received: 18.12.2018.

Accepted: 20.02.2019.



# ONE-POT GREEN SYNTHESIS OF 3-AMINO-1-(5-NITRO-1H-INDOL-2-YL)-5,10-DIOXO-5,10-DIHYDRO-1H-PYRAZOLO[1,2-*b*]PHTHALAZINE-2-CARBONITRILE AND RELATED COMPOUNDS

Rama Koteswar Rao<sup>[a]\*</sup> and Shravankumar Kankala<sup>[a]</sup>

**Keywords:** Eco-friendly synthesis; One-pot reaction; pyrazolo[1,2-*b*]phthalazine; glycerol; triethylamine catalyst.

Synthesis of 3-amino-1-(5-nitro-1H-indol-2-yl)-5,10-dioxo-5,10-dihydro-1H-pyrazolo[1,2-*b*]phthalazine-2-carbonitriles by a one-pot green and an eco-friendly reaction of phthalic acid, hydrazine hydrate, indole-3-carboxaldehydes and malononitrile/ethyl cyanoacetate in the presence of Et<sub>3</sub>N as catalyst and Glycerol mediated at 100-105 °C for 45-60 min. This one-pot reaction proceeded in a short time with good yields and the desired products obtained without using column purifications.

\* Corresponding Authors

E-Mail: ramakdcj99@gmail.com

[a] Mewar University, Chittorgarh, Rajasthan, India- 312901

## INTRODUCTION

Multi-component reactions (MCRs) are one-pot processes in which three or more compounds react in a single reaction vessel to form a product containing substantial components of all the reactants.<sup>1</sup> Thus, design of highly efficient chemical reaction sequences that provide maximum structural complexity and diversity with a minimum number of steps in the synthesis of compounds with interesting properties is essential for drug discovery and synthesis of natural products.<sup>2</sup> MCRs have attracted much attention in combinatorial and medicinal chemistry and have been designed to produce biologically active compounds.<sup>3,4</sup>

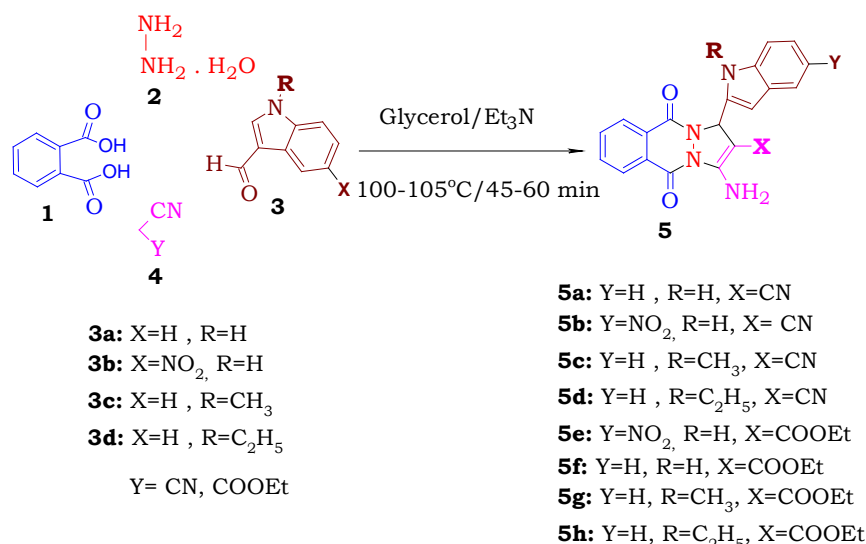
Phthalazines are important heterocycles that are known to possess multiple biological activities such as antimicrobial, anticonvulsant, antifungal, anticancer and anti-inflammatory.<sup>5</sup> Carling et al. reported<sup>6</sup> the synthesis of 3-phenyl-6-(2-pyridyl)methoxy-1,2,4-triazolo[3,4-*a*]phthalazines and analogs which were found to be a critical structural element of specific CNS - active drugs. Jain et al. reported<sup>7</sup> the synthesis of keto-glutamine tetrapeptide analogs containing a 2-oxopyrrolidine ring as a glutamine side chain mimic which showed improved inhibition against hepatitis A virus 3C proteinase. Grasso et al. reported<sup>8</sup> the synthesis of 6,7-methylenedioxyphtalazin-1(2H)-ones which were found to be potent anticonvulsant agents. Nomoto et al. reported<sup>9</sup> the synthesis of 6,7-dimethoxyphthalazine derivatives which showed relatively potent cardiotoxic activity comparable to that of amrinone. Watanabe et al. reported<sup>10</sup> the synthesis of 4-benzylamino-1-chloro-6-substituted phthalazines which were found to be vasorelaxant and some methods have been reported for the synthesis of phthalazine derivatives.<sup>11</sup> Therefore, it was considered worthwhile to synthesize phthalazine moiety containing 4H-pyrans.

Keeping above discussion in our mind, we now wish to report 3-amino-1-(5-nitro-1H-indol-2-yl)-5,10-dioxo-5,10-dihydro-1H-pyrazolo[1,2-*b*]phthalazine-2-carbonitrile derivatives by reaction of phthalic acid, hydrazine hydrate, indole-3-carboxaldehydes and malononitrile/ethyl cyanoacetate in the presence of Et<sub>3</sub>N as catalyst and glycerol as a medium at 100-105 °C for 30-60 min.

## RESULTS AND DISCUSSION:

Firstly, we have initiated the optimization of the one-pot four-component reaction by using phthalic acid (**1**) and hydrazine hydrate (**2**) to in-situ formation of phthalic hydrazide as intermediate in the presence of Et<sub>3</sub>N and glycerol medium. To this reaction mixture, 5-nitroindole-3-carboxaldehyde (**3a**) and malononitrile (**4a**) were added for preparation of 3-amino-1-(5-nitro-1H-indol-2-yl)-5,10-dioxo-5,10-dihydro-1H-pyrazolo[1,2-*b*]phthalazine-2-carbonitrile (**5a**) in the presence of different solvents (glycerol, ethylene glycol and DMF) and different bases (Et<sub>3</sub>N and pyridine) at different temperature (RT, 50 °C, 100 °C and 120 °C) as a simple model reaction (Table 1 entries 1–3). However, it was found that the one-pot reaction of **1** (10 mM), **2** (10 mM), **3a** (10 mM) and **4a** (10 mM) in the presence of Et<sub>3</sub>N (2 mM) as catalyst and glycerol (50 ml) as medium for 45 min at 100 °C gave the highest yield (88 %) and clean product (**5a**) (Table 1, entry 1). <sup>1</sup>H-NMR, IR and mass spectroscopy have confirmed the structure of the compound **5a**.

In order to examine the quantity of Et<sub>3</sub>N, the one-pot reaction has been carried out at different quantity (1 mM, 2 mM and 5 mM) of Et<sub>3</sub>N with respect of phthalic acid **1**. However, it was found that the one-pot reaction of **1** (10 mM), **2** (10 mM), **3a** (10 mM) and **4a** (10 mM) in the presence of Et<sub>3</sub>N (2 mM) as catalyst and glycerol medium (50 ml) for 45 min at 100-105 °C gave the highest yield (88 %) (Table 2, entry 2).



**Scheme 1.** The general reaction route to prepare the pyrazolo[1,2-b]phthalazine derivatives

In the next step, the scope of the reaction process was explored, using the best-optimized conditions by changing the phthalic acid, the aldehyde & the nitrile (Table 3). The results are displayed in Table 3. The structures of the products were assigned on the basis of their spectral properties - IR, NMR and mass spectra (for details, please see the experimental section).

**Table 1.** Effect of solvent/catalyst and temperature on the one-pot reaction of 1, 2, 3a and 4a at RT yielding 5a.

No.	Solvent/Catalyst	T, °C	Time, min	Yield 5a, %
1	Glycerol/Et <sub>3</sub> N	100	45	88
2	Ethylene glycol /Et <sub>3</sub> N	100	55	80
3	DMF/Et <sub>3</sub> N	100	100	80
4	Glycerol/pyridine	100	40	80
5	Ethylene glycol/pyridine	100	50	78
6	DMF/pyridine	100	90	72
7	Glycerol/Et <sub>3</sub> N	RT	300	85
8	Ethylene glycol/Et <sub>3</sub> N	RT	320	82
9	DMF/Et <sub>3</sub> N	RT	450	78
10	Glycerol/Et <sub>3</sub> N	50	80	82
11	Ethylene glycol/Et <sub>3</sub> N	50	85	81
12	DMF/Et <sub>3</sub> N	50	100	79
13	Glycerol/Et <sub>3</sub> N	120	40	75
14	Ethylene glycol/Et <sub>3</sub> N	120	45	70
15	DMF/Et <sub>3</sub> N	120	60	73

A schematic mechanism for the catalytic activity of Et<sub>3</sub>N in the synthesis of titled compounds **5** can be postulated as shown in Scheme 2. This mechanism contains three steps. In the first step, the formation of phthalic hydrazide (**X1**) by nucleophilic addition of hydrazine hydrate (**2**) to phthalic acid (**1**) takes place followed by dehydration. The second step involves forming heterodiene (**Y1**) by standard Knoevenagel condensation of indole-3-carboxaldehyde (**3**) and malononitrile/ethyl cyanoacetate (**4**). Then, in the third step, Michael-type addition of the phthalic hydrazide **X1** to

heterodiene **Y1** takes place forming the intermediary iminomethylene derivative **Z** which undergoes cyclisation affording **5**.

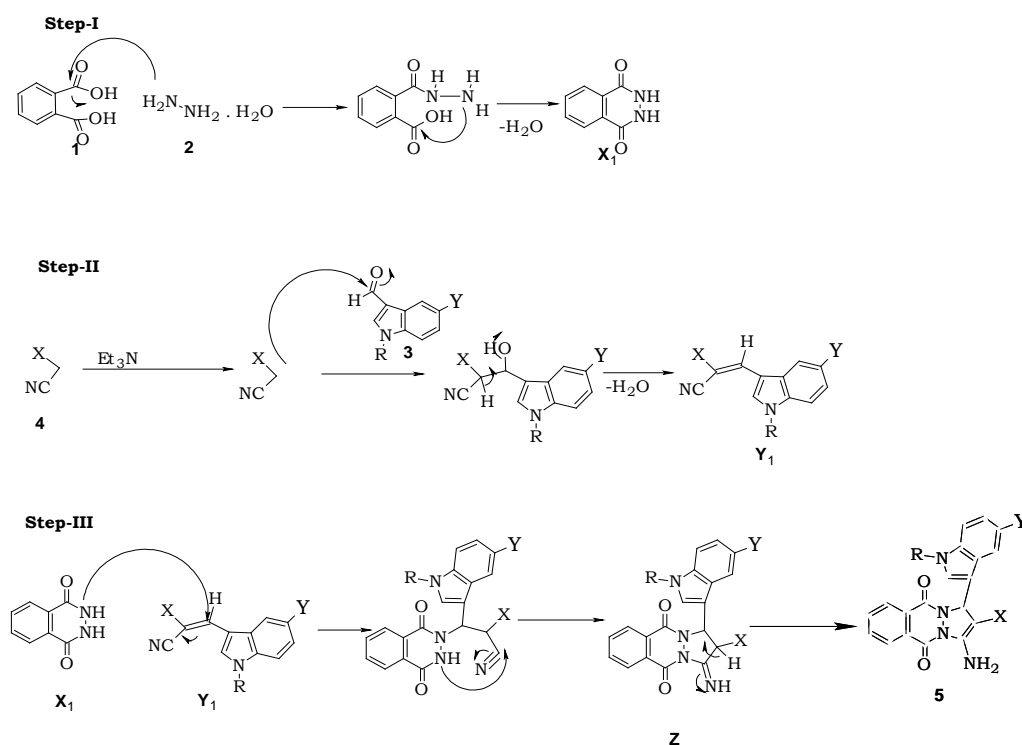
**Table 2.** Effect of Et<sub>3</sub>N catalyst quantity on the one-pot reaction of 1, 2, 3a and 4a at 100-105 °C yielding 5a in glycerol.

No.	Catalyst concentration	T, °C	Time, min	Yield, 5a, %
1	1 mM	100	120	75
2	2 mM	100	45	88
3	5 mM	100	40	78

**Table 3.** Characterization data, reaction time and yields of **5** obtained from **1**, **2**, **3** and **4** via one-pot, four component synthesis.

Starting materials (1, 2, 3 and 4)	Product	Time, min	Yield, %
<b>3a</b> (R=H, Y=NO <sub>2</sub> )	<b>4a</b> (X=CN)	<b>5a</b>	45 88
<b>3b</b> (R=H, Y=H)	<b>4a</b> (X=CN)	<b>5b</b>	48 86
<b>3c</b> (R=CH <sub>3</sub> , Y=H)	<b>4a</b> (X=CN)	<b>5c</b>	50 85
<b>3d</b> (R=C <sub>2</sub> H <sub>5</sub> , Y=H)	<b>4a</b> (X=CN)	<b>5d</b>	55 84
<b>3a</b> (R=H, Y=NO <sub>2</sub> )	<b>4b</b> (X=COOEt)	<b>5e</b>	50 87
<b>3b</b> (R=H, Y=H)	<b>4b</b> (X=COOEt)	<b>5f</b>	60 86
<b>3c</b> (R=CH <sub>3</sub> , Y=H)	<b>4b</b> (X=COOEt)	<b>5g</b>	60 84
<b>3d</b> (R=C <sub>2</sub> H <sub>5</sub> , Y=H)	<b>4b</b> (X=COOEt)	<b>5h</b>	60 86

≠ Refers to yields of crude products only.



**Scheme 2.** A plausible mechanism for **5** from **1**, **2**, **3** and **4**.

## EXPERIMENTAL SECTION

Melting points are uncorrected and were determined in open capillary tubes in a sulphuric acid bath. TLC was run on silica gel-G and visualization were done using iodine vapor or UV light. IR spectra were recorded using a Perkin-Elmer 1000 instrument in KBr pellets.  $^1\text{H}$  NMR spectra were recorded in DMSO- $d_6$  using TMS as an internal standard at 400 MHz operating frequency. Mass spectra were recorded on an Agilent-LC-MS instrument.

### General procedure for preparation of **5**

Phthalic acid (**1**) (10 mM) and hydrazine hydrate (**2**) (10 mM) were charged in glycerol (50 ml) in the presence of  $\text{Et}_3\text{N}$  (3 mM) and heated for 10 min at 100-105  $^\circ\text{C}$  to form phthalic acid hydrazide. Then, 5-nitroindole-3-carboxaldehydes (**3a**) (10 mM) and malononitrile/ethylcyanoacetate (**4**) (10 mM) were added to this reaction mixture and again heated for 20-35 min (until no starting materials could be detected on thin-layer chromatography). After the reaction was completed, cold water was added to the reaction mixture and solid part was separated by filtration. The product was recrystallised from ethanol solvent to obtain **5**.

### 3-Amino-1-(5-nitro-1H-indol-2-yl)-5,10-dioxo-5,10-dihydro-1H-pyrazolo[1,2-*b*]phthalazine-2-carbonitrile (**5a**)

M.p.: >220  $^\circ\text{C}$ ; IR (KBr): 3116-3440  $\text{cm}^{-1}$  (broad, medium, -NH group), 2218 (sharp, strong, -CN group), 1669  $\text{cm}^{-1}$

(sharp, strong, -CO of amide group), 1686  $\text{cm}^{-1}$  (sharp, strong, -CO of amide group);

$^1\text{H}$ -NMR (DMSO- $d_6$ , 400 MHz):  $\delta$  5.67 (s, 1H, -CH), 7.26-8.68 (m, 10H, Ar-H and  $\text{NH}_2$ ),  $\delta$  11.87 (s, 1H, -NH);  $^{13}\text{C}$ -NMR (DMSO- $d_6$ , 100 MHz):  $\delta$  61.5, 69.1, 110.6, 111.5, 115.8, 115.9, 119.2, 122.9, 123.6, 127.6, 134.6, 135.6, 138.4, 144.6, 145.8, 161.6, 164.5;  $[\text{M}+\text{H}]^+$ : 400

### 3-Amino-1-(1H-indol-2-yl)-5,10-dioxo-5,10-dihydro-1H-pyrazolo[1,2-*b*]phthalazine-2-carbonitrile (**5b**)

M.p.: >220  $^\circ\text{C}$ ; IR (KBr): 3116-3440  $\text{cm}^{-1}$  (broad, medium, -NH group), 2218 (sharp, strong, -CN group), 1669  $\text{cm}^{-1}$  (sharp, strong, -CO of amide group), 1686  $\text{cm}^{-1}$  (sharp, strong, -CO of amide group);  $^1\text{H}$ -NMR (DMSO- $d_6$ , 400 MHz):  $\delta$  5.67 (s, 1H, -CH), 7.26-8.68 (m, 11H, Ar-H and  $\text{NH}_2$ ),  $\delta$  11.87 (s, 1H, -NH);  $^{13}\text{C}$ -NMR (DMSO- $d_6$ , 100 MHz):  $\delta$  61.0, 69.0, 110.1, 111.5, 115.9, 119.2, 122.9, 123.9, 127.3, 134.6, 135.8, 138.4, 144.6, 145.8, 161.0, 164.5;  $[\text{M}+\text{H}]^+$ : 356

### 3-Amino-1-(1-methyl-1H-indol-2-yl)-5,10-dioxo-5,10-dihydro-1H-pyrazolo[1,2-*b*]phthalazine-2-carbonitrile (**5c**)

M.p.: >220  $^\circ\text{C}$ ; IR (KBr) 2213 (sharp, strong, -CN group), 1668  $\text{cm}^{-1}$  (sharp, strong, -CO- of amide group), 1682  $\text{cm}^{-1}$  (sharp, strong, -CO of amide group);  $^1\text{H}$ -NMR (DMSO- $d_6$ , 400 MHz):  $\delta$  2.20 (s, 3H, - $\text{CH}_3$ ), 5.30 (s, 1H, -CH), 7.21-8.68 (m, 11H, Ar-H and  $\text{NH}_2$ );  $^{13}\text{C}$ -NMR (DMSO- $d_6$ , 400 MHz):  $\delta$  23.4, 60.1, 68.1, 111.3, 111.4, 114.8, 118.1, 122.9,

123.6, 127.4, 133.5, 134.7, 138.3, 144.2, 145.9, 161.4, 164.4; [M+H]<sup>+</sup>: 370

**3-Amino-1-(1-ethyl-1H-indol-2-yl)-5,10-dioxo-5,10-dihydro-1H-pyrazolo[1,2-*b*]phthalazine-2-carbonitrile (5d)**

M.p.: >220 °C; IR (KBr) 2216 (sharp, strong, -CN group), 1663 cm<sup>-1</sup> (sharp, strong, -CO of amide group), 1678 cm<sup>-1</sup> (sharp, strong, -CO of amide group); <sup>1</sup>H-NMR (DMSO-d<sub>6</sub>, 400 MHz): δ 1.81 (t, 3H, CH<sub>3</sub>), 2.22 (q, 2H, -CH<sub>2</sub>), 5.26 (s, 1H, -CH), 7.21-8.94 (m, 11H, Ar-H and NH<sub>2</sub>); <sup>13</sup>C-NMR (DMSO-d<sub>6</sub>, 400 MHz): δ 19.2, 23.2, 60.4, 68.5, 111.2, 111.5, 114.2, 118.2, 122.4, 123.2, 127.1, 133.0, 134.3, 138.2, 144.0, 145.2, 161.5, 164.9; [M+H]<sup>+</sup>: 384

**Ethyl-3-amino-1-(5-nitro-1H-indol-2-yl)-5,10-dioxo-5,10-dihydro-1H-pyrazolo[1,2-*b*]phthalazine-2-carboxylate (5e)**

M.p.: >220 °C; IR (KBr): 3076-3360 cm<sup>-1</sup> (broad, medium, -NH group), 2297 (sharp, strong, -CN group), 1660 cm<sup>-1</sup> (sharp, strong, -CO of amide group), 1666 cm<sup>-1</sup> (sharp, strong, -CO of amide group); <sup>1</sup>H NMR (DMSO-d<sub>6</sub>, 400 MHz): δ 1.32 (t, 3H, -CH<sub>3</sub>), 4.46 (q, 2H, -CH<sub>2</sub>), 6.02 (s, 1H, -CH), 7.20-8.69 (m, 10H, Ar-H and NH<sub>2</sub>), δ 11.79 (s, 1H, -NH); <sup>13</sup>C-NMR (DMSO-d<sub>6</sub>, 400 MHz): δ 14.0, 61.9, 69.1, 74.0, 110.6, 111.1, 115.8, 115.9, 119.1, 122.9, 123.6, 127.1, 134.6, 135.7, 140.6, 143.7, 151.6, 155.6; [M+H]<sup>+</sup>: 402

**Ethyl-3-amino-1-(1H-indol-2-yl)-5,10-dioxo-5,10-dihydro-1H-pyrazolo[1,2-*b*]phthalazine-2-carboxylate (5f)**

M.p.: >220 °C; IR (KBr): 3112-3453 cm<sup>-1</sup> (broad, medium, -NH group), 2204 (sharp, strong, -CN group), 1668 cm<sup>-1</sup> (sharp, strong, -CO of amide group), 1672 cm<sup>-1</sup> (sharp, strong, -CO of amide group); <sup>1</sup>H NMR (DMSO-d<sub>6</sub>, 400 MHz): δ 1.24 (t, 3H, -CH<sub>3</sub>), 4.18 (q, 2H, -CH<sub>2</sub>), 5.42 (s, 1H, -CH), 7.22-8.68 (m, 11H, Ar-H and NH<sub>2</sub>), δ 11.78 (s, 1H, -NH); <sup>13</sup>C NMR (DMSO-d<sub>6</sub>, 400 MHz): δ 15.3, 55.2, 60.5, 68.1, 110.3, 111.4, 115.0, 117.2, 122.0, 123.5, 127.2, 133.0, 134.9, 137.3, 142.5, 144.5, 150.1, 156.4; [M+H]<sup>+</sup>: 403

**Ethyl-3-amino-1-(1-methyl-1H-indol-2-yl)-5,10-dioxo-5,10-dihydro-1H-pyrazolo[1,2-*b*]phthalazine-2-carboxylate (5g)**

M.p.: >220 °C; IR (KBr) 2213 (sharp, strong, -CN group), 1664 cm<sup>-1</sup> (sharp, strong, -CO of amide group), 1683 cm<sup>-1</sup> (sharp, strong, -CO of amide group); <sup>1</sup>H NMR (DMSO-d<sub>6</sub>, 400 MHz): δ 1.12 (t, 3H, -CH<sub>3</sub>), 2.24 (s, 3H, -CH<sub>3</sub>), 4.00 (q, 2H, -CH<sub>2</sub>), 5.42 (s, 1H, -CH), 7.22-8.64 (m, 11H, Ar-H and NH<sub>2</sub>); <sup>13</sup>C NMR (DMSO-d<sub>6</sub>, 400 MHz): δ 15.3, 22.5, 56.3, 61.4, 67.0, 111.4, 113.5, 114.7, 118.0, 122.0, 122.7, 125.0, 132.4, 134.6, 138.0, 144.1, 143.5, 152.2, 153.5; [M+H]<sup>+</sup>: 417

**Ethyl-3-amino-1-(1-ethyl-1H-indol-2-yl)-5,10-dioxo-5,10-dihydro-1H-pyrazolo[1,2-*b*]phthalazine-2-carboxylate (5h)**

M.p.: >220 °C; IR (KBr): 2215 cm<sup>-1</sup> (sharp, strong, -CN group), 1666 cm<sup>-1</sup> (sharp, strong, -CO of amide group),

1673 cm<sup>-1</sup> (sharp, strong, -CO of amide group); <sup>1</sup>H NMR (DMSO-d<sub>6</sub>, 400 MHz): δ 1.18 (t, 3H, -CH<sub>3</sub>), 1.69 (t, 3H, CH<sub>3</sub>), 2.39 (q, 2H, -CH<sub>2</sub>), 4.15 (q, 2H, -CH<sub>2</sub>), 5.26 (s, 1H, -CH), 7.22-8.93 (m, 11H, Ar-H and NH<sub>2</sub>); <sup>13</sup>C NMR (DMSO-d<sub>6</sub>, 400 MHz): δ 15.2, 19.4, 23.6, 54.3, 60.2, 68.4, 111.5, 111.7, 114.0, 118.1, 122.3, 124.1, 126.8, 133.4, 134.9, 138.1, 144.2, 145.5, 151.6, 154.6; [M+H]<sup>+</sup>: 431

## CONCLUSION

In summary, a novel method to prepare 3-amino-1-(5-nitro-1H-indol-2-yl)-5,10-dioxo-5,10-dihydro-1H-pyrazolo[1,2-*b*]phthalazine-2-carbonitrile and related derivatives have been developed by the reaction of phthalic acid, hydrazine hydrate, indole-3-carboxaldehydes and malononitrile/ethyl cyanoacetate in the presence of Et<sub>3</sub>N and glycerol mediated at 100-105 °C for 30-60 min. This one-pot reaction proceeds in a short time with good yields and the desired products obtained without using column chromatographic purifications.

## Acknowledgment

The authors would like to thank Mewar University, Rajasthan for permitting the research work and for constant encouragement.

## REFERENCES

- Montagne, C., Shiers, J. J., Shipman, M. Rapid generation of molecular complexity using "sequenced" multi-component reactions: one-pot synthesis of 5,5'-disubstituted hydantoins from methyleneaziridines, *Tetrahedron Lett.* **2006**, *47*, 9207. <https://doi.org/10.1016/j.tetlet.2006.10.135>
- Bienayme, H.; Multicomponent Reactions, Wiley-VCH, Weinheim, **2005**, 311-341. <https://doi.org/10.1016/j.tetlet.2006.10.135>
- Braese, S., Gil, C., Knepper, K. The recent impact of solid-phase synthesis on medicinally relevant benzoannulated nitrogen heterocycles, *Bioorg. Med. Chem.* **2002**, *10*, 2415. [https://doi.org/10.1016/S0968-0896\(02\)00025-1](https://doi.org/10.1016/S0968-0896(02)00025-1)
- Hailes, H. C., Reaction Solvent Selection: The Potential of Water as a Solvent for Organic Transformations, *Org. Process Res. Dev.*, **2007**, *11*, 114. DOI: 10.1021/op060157x
- El-Sakka, S. S.; Soliman, A. H.; Imam, A. M., Synthesis, antimicrobial activity and Electron Impact of Mass Spectra of Phthalazine-1,4-dione Derivatives, *Afinidad.* **2009**, *66*, 167. <https://core.ac.uk/download/pdf/39152404.pdf>
- Carling, R. W., Moore, K. W., Street, L. J., Wild, D., Isted, C., Leeson, P. D., Thomas, S., O'Connor, D., McKernan, R. M., Quirk, K., Cook, S. M., Atack, J. R., Waftord, K. A., Thompson, S. A., Dawson, G. R., Ferris, P., Castro, J. L., 3-Phenyl-6-(2-pyridyl)methoxy-1,2,4-triazolo[3,4-*a*]phthalazines and Analogues: High-Affinity  $\gamma$ -Aminobutyric Acid-A Benzodiazepine Receptor Ligands with  $\alpha$ 2,  $\alpha$ 3, and  $\alpha$ 5-Subtype Binding Selectivity over  $\alpha$ 1, *J. Med. Chem.* **2004**, *47*, 1807; DOI: 10.1021/jm031020p
- Jain, R., Vederas, J. C., Structural variations in keto-glutamines for improved inhibition against hepatitis A virus 3C proteinase, *Bioorg. Med. Chem. Lett.* **2004**, *14*, 3655. <https://doi.org/10.1016/j.bmcl.2004.05.021>
- Grasso, S., DeSarro, G., Micale, N., Zappala, M., Puia, G., Baraldi, M., Demicheli, C., Synthesis and Anticonvulsant Activity of Novel and Potent 6,7-Methylenedioxyphthalazin-

- 1(2*H*)-ones, *J. Med. Chem.* **2000**, *43*, 2851; DOI: [10.1021/jm001002x](https://doi.org/10.1021/jm001002x)
- <sup>9</sup>Nomoto, Y., Obase, H., Takai, H., Teranishi, M., Nakamura, J., Kubo, K., Studies on Cardiotonic Agents. II.: Synthesis of Novel Phthalazine and 1,2,3-Benzotriazine Derivatives, *Chem. Pharm. Bull. (Tokyo)* **1990**, *38*, 2179. <https://doi.org/10.1248/cpb.38.2179>
- <sup>10</sup>Watanabe, N., Kabasawa, Y., Takase, Y., Matsukura, M., Miyazaki, K., Ishihara, H., Kodama, K., Adachi, H., 4-Benzylamino-1-chloro-6-substituted Phthalazines: Synthesis and Inhibitory Activity toward Phosphodiesterase 5, *J. Med. Chem.* **1998**, *41*, 3367. DOI: [10.1021/jm970815r](https://doi.org/10.1021/jm970815r)
- <sup>11</sup>Sheradsky, T., Moshenberg, R., Bridgehead hydrazines. Unusual photorearrangement of 1,4-diphenylpyridazino[1,2-b]phthalazine-6,11-dione, *J. Org. Chem.* **1986**, *51*, 3123. DOI: [10.1021/jo00366a008](https://doi.org/10.1021/jo00366a008)

Received: 20.12.2018.

Accepted: 26.02.2019.



# SYNTHESIS OF GRAPHENE OXIDE AND REDUCED GRAPHENE OXIDE FROM INDUSTRIAL GRAPHITE FOIL WASTES

N. G. Barbakadze,<sup>[a]\*</sup> V. G. Tsitsishvili,<sup>[a]</sup> T. V. Korkia,<sup>[a]</sup> Z. G. Amiridze,<sup>[a]</sup> N. V. Jalabadze<sup>[b]</sup> and R.V. Chedia<sup>[a]</sup>

**Keywords:** graphite foil wastes, Hummers method, graphene oxide, reduced graphene oxide

Powdered graphite foil wastes (pGFW) were successfully used for the synthesis of graphene oxide (GO) and reduced graphene oxide (rGO). The remaining graphite foil pieces (wastes) are expanded graphites and their chemical oxidation to GO or to obtain graphene can be conducted using known methods. A fraction with a particle size of  $<140\ \mu\text{m}$  was obtained by wet and dry grinding. The EDX analysis showed that the powder consists of carbon and oxygen only. The paper presents results obtained in pGF oxidation using low-temperature ( $\sim 0^\circ\text{C}$ ;  $\text{KMnO}_4\text{-NaNO}_3\text{-H}_2\text{SO}_4$ ) and relatively high-temperature ( $\sim 50^\circ\text{C}$ ;  $\text{KMnO}_4\text{-H}_2\text{SO}_4$ ) modes. In case of low-temperature mode oxidation of pGFW the C/O ratio (at.%) is 61:38. In case of their reduction with ascorbic acid the C/O ratio is 81:19. The method of synthesis of GO and its separation from the reaction mixture were partially corrected. Sulfuric acid and ions ( $\text{K}^+$ ,  $\text{Na}^+$ , and  $\text{Mn}^{+2}$ ) can be removed using 5-fold decanting (2 times  $\text{H}_2\text{O}$ , 3 times 5% HCl solution). A 5 % solution of HCl precipitates GO-flakes in 7–10 min and, thus, the process of removing the main impurities is accelerated. From decanted solutions, GO was reduced to the rGO with ascorbic acid at  $80^\circ\text{C}$ . By the high-temperature treatment of rGO received from graphite foil wastes graphene is obtained with a defective structure.

\* Corresponding Author

E-Mail: chemicalnatia@yahoo.de

- [a] Laboratory of Problems of Chemical Ecology, Petre Melikishvili Institute of Physical and Organic Chemistry, Tbilisi State University, Tbilisi, Georgia, e-mail: chemicalnatia@yahoo.de
- [b] Republic Center for Structure Researches of Georgia, Georgian Technical University, Tbilisi, Georgia, e-mail: jalabadze@gtu.ge

## Introduction

Due to their unique physical-chemical properties, use of compounds with carbon 2D and 3D structures are great importance and perspective. The graphene oxide (GO) and the reduced graphene oxide (rGO) are graphite graphene-monolayer oxidation products that have organic functional groups; therefore their future functionalization or joining (immobilization) in organic or inorganic precursors may be performed. There are many organic–organic, organic–inorganic, inorganic–inorganic composites containing graphene structures and they have a wide area of application. Both, natural and synthetic graphite can be used to prepare these materials, but the natural graphite is cheaper, therefore the natural flake graphite powders with a particle size of less than  $400\ \mu\text{m}$  are mostly used in industry or laboratory practice. Purification of the natural graphite from impurities is carried out by separation or flotation, chemical processing. For example, by the enrichment of raw ore containing 68% C graphite is obtained after enrichment with 97.68% C graphite content, which can be used in the synthesis of GO and rGO.<sup>1</sup> Thorough cleaning of graphite is necessary, because the impurities in it could be found in targeted products.<sup>2</sup>

In general, GO and rGO structural-morphological properties depend on the used graphite nature, powder particles size, oxidation and reduction methods, thermal treatment conditions, etc. Accordingly, GO and rGO physical-mechanical properties or chemical composition changes within a wide range. The use of different precursors of graphite for GO synthesis is discussed in many scientific sources.<sup>3</sup> Dependence of oxidation degree, hydrophilicity and microstructure of GO prepared on nature of graphite precursors were studied with using flake expandable and microcrystalline graphite precursors. It is estimated that the GO prepared on the basis of expandable graphite is characterized by a higher degree of oxidation than in case of microcrystalline graphite.<sup>4</sup>

GO could be obtained by a modified Hummers method from synthetic graphite powders. The graphite powder SP-1 was washed with NaCl solution, then oxidized with  $\text{KMnO}_4\text{-H}_2\text{SO}_4$  at low temperatures ( $<20^\circ\text{C}$ ).<sup>5</sup> For the synthesis of GO it was successfully used expanded graphite. The process of synthesis was done below  $<20^\circ\text{C}$  in  $\text{KMnO}_4\text{-H}_2\text{SO}_4$  system [6]. In contrast to other works, GO could also be extracted from low-grade coal and wood charcoal. Extraction was conducted with the dilute nitric acid and by the neutralization of extract with sodium hydroxide. Obtained GO is used in Alzheimer drug encapsulation.<sup>7</sup>

One of the interesting methods for GO synthesis is the improved Hummers method, where flake graphite oxidation is performed with  $\text{KMnO}_4\text{-H}_2\text{SO}_4\text{-H}_3\text{PO}_4$  mixture at  $50^\circ\text{C}$  and at a ratio of  $\text{H}_2\text{SO}_4/\text{H}_3\text{PO}_4 = 9:1$ <sup>8</sup>, and the optimized conditions led to GO in 3 h.

GO and rGO could also be obtained from commercial expanded graphite with grain size  $D_{50} \sim 15 \mu\text{m}$ . GO was obtained by a new modified Hummers method. At the initial stage the powder of graphite and potassium permanganate is mixed, cooled and then 98 % sulfuric acid is added.<sup>10</sup> The synthesis ends in a relatively short period of time since the particles of the graphite powder used were small.

Expanded graphite was also used in 10–30  $\mu\text{m}$  size.<sup>1</sup> The synthesis was conducted using ultrasonic cleaner used after the reaction is terminated with water (90 °C, 10 min). Thus, for obtaining of the GO and rGO, natural and synthetic graphites, graphite intercalated with different compounds and expanded graphite can also be used. It is established that the reduction of the GO obtained from the samples of the different types of graphite are formed graphenes, in which the number of layers was very different (1–10 layers or more).<sup>12–16</sup>

Flexible graphite foils in various thickness and width are used in modern technologies (chemical, petrochemical, metallurgical processes, for the production of ceramic composites).<sup>17</sup> The remaining graphite foil pieces (wastes) are expanded graphites, and their chemical oxidation to GO or to obtain graphene can be conducted using known methods with some adjustments.<sup>18</sup> The purpose of the present work is studying on the usability of wastes of the graphite foils as the precursors for GO and rGO synthesis.

## Experiments

Flake graphite,  $\text{KMnO}_4$ ,  $\text{NaNO}_3$ ,  $\text{H}_2\text{SO}_4$  (98 %),  $\text{HCl}$  (37 %),  $\text{HI}$  (57 %) and ascorbic acid were purchased from Sigma Aldrich. The morphology of the samples was studied by optical and scanning electron microscopes (Nikon ECLIPSE LV 150, LEITZ WETZLAR and JEOL JSM-6510 LV-SEM). Samples X-ray diffraction (XRD) patterns were obtained with a DRON-3M diffractometer ( $\text{Cu-K}\alpha$ , Ni filter,  $2^\circ/\text{min}$ ). After purification, graphite foil powders were analyzed using EDS.

### Obtaining of powdered graphite foil wastes (pGFW)

The initial powders were obtained by grinding of flake wastes in water (blender). After drying the powder, that was still dry ground using a laboratory mill. Removal of impurities from the powders was carried out with chemical reagents and their subsequent sifting fractions with particles  $<140 \mu\text{m}$  were collected. From these powders, the graphene oxide was obtained with different oxidation systems ( $\text{KMnO}_4\text{-NaNO}_3\text{-H}_2\text{SO}_4$  and  $\text{KMnO}_4\text{-H}_2\text{SO}_4$ ).

### Graphene oxide synthesis with Hummers method

In details, 0.75g  $\text{NaNO}_3$  and 80ml of 98% sulfuric acid were added to 1 g of pGFW. The reaction mixture was cooled up to  $-2 - +1^\circ\text{C}$  and stirred for 30 min. Over the next 50 min, 6 g of  $\text{KMnO}_4$  was added. The temperature was left to raise until room temperature (3 h) during stirring, and the mixture was further stirred for half an hour at  $35\text{--}40^\circ\text{C}$ . The reaction mixture was diluted with 100 ml of cold water, keeping the temperature below  $90^\circ\text{C}$ , and then stirred at this

temperature for 30 min. The mixture was diluted to 300 ml. Residual amount of potassium permanganate was removed by 3 % hydrogen peroxide solution. A yellowish suspension of graphite oxide was obtained, its color gradually changed to dark brown.

The resulting suspension was left to stand for 20 min, then the precipitate was removed by decantation. This operation was repeated twice. For the rapid precipitation of graphene oxide from the suspension, a 5 % solution of hydrochloric acid (300 ml) was added. Decantation was repeated 3 times in 10 min intervals. An aqueous gel-like mass was obtained by centrifuging and washing the sediment, the pH was between 5 and 6. The sediment was washed with acetone 3 times and is dried in vacuum at  $70^\circ\text{C}$  for 4 h. The decanted solutions contained 12–17 wt.% of GO. Its reduction to the rGO was conducted with ascorbic acid. For this purpose, the decanted solutions were mixed with 1 g of ascorbic acid and heated until  $80^\circ\text{C}$ . The brown solution darkens rapidly due to the formation of reduced graphene oxide. rGO precipitation occurred when the reaction mixture was cooled (10 min). The precipitate was filtered, washed with sodium bicarbonate solution, then with water until reaching  $\text{pH} = 6$ , acetone (x3) and dried in vacuum at  $70^\circ\text{C}$ .

### Oxidation of pGFW with $\text{KMnO}_4\text{-H}_2\text{SO}_4$ system

For oxidation of pGFW, we used a simplified oxidation system of  $\text{KMnO}_4\text{-H}_2\text{SO}_4$ .<sup>9</sup> In more details, 40 ml of 98 % sulfuric acid is added to 1 g pGFW ( $<140 \mu\text{m}$ ) in a glass reactor. The mixture was stirred at  $35\text{--}40^\circ\text{C}$  for half an hour and 3 g of potassium permanganate was added at  $40\text{--}45^\circ\text{C}$  under 1 h (the temperature can reach  $50^\circ\text{C}$ ). The mixture was stirred for 3 h. A gray viscous mass was obtained, which was cooled to  $10^\circ\text{C}$  and 100 ml of ice-water was added to the glass reactor. A sharp change in the temperature of the reaction mixture was not observed while adding the water. After adding 3–4 drops of hydrogen peroxide (30 %), the reaction mixture becomes sharp yellow. Isolation of graphene oxide from the suspension and receiving of rGO from decanted solutions was carried out using the way mentioned above.

## Results and discussion

Graphite foil wastes from various technological processes are contaminated with various types of organic and inorganic compounds which can be removed with various methods after grinding the waste. The graphite foil wastes used in our experiments contained about 6% oxygen and some other elements as well (Figure 1). After their wet grinding, a powder with a particle size of  $<1 \text{ mm}$  was obtained, and the amount of fine fraction ( $<50 \mu\text{m}$ ) does not exceed 6–8 %. In the case of dry grinding of these powders, a fraction with a particle size of  $<140 \mu\text{m}$  could be obtained, which was treated with various reagents to remove the impurities. As the EDX analysis showed, the powder produced consisted of carbon and oxygen (Figure 2).

The SEM image shows that each particle of the powder is composed of layers rolled on each other and had different forms. The thickness of the sheets were found to be  $\sim 0.5 \mu\text{m}$  (Figures 1 and 2).





**Figure 1.** Graphite foil wastes (I) and pGFW (II).

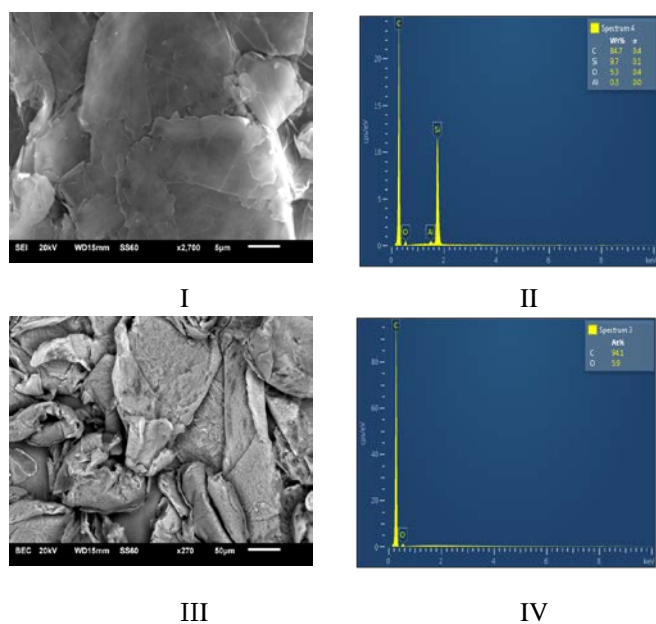


**Figure 2.** SEM image (I and III) and EDX spectrum (II and IV) of pGFW and purified (chemically) pGFW

Oxidizing reagents can easily penetrate the layers and intercalation or functionalization-oxidation processes can be occurred resulting in graphene oxide. Using of pGFW with a particle size of 200–500  $\mu\text{m}$  to prepare of GO and the rGO may also be possible.

The GO synthesis from pGFW was conducted using the same methods as in case of other types of graphite precursors. The  $\text{KMnO}_4\text{-H}_2\text{SO}_4$  and  $\text{KMnO}_4\text{-NaNO}_3\text{-H}_2\text{SO}_4$  systems were tested in the pGFW oxidation using low-temperature ( $\sim 0^\circ\text{C}$ ;  $\text{KMnO}_4\text{-NaNO}_3\text{-H}_2\text{SO}_4$ ) and relatively high-temperature ( $\sim 50^\circ\text{C}$ ;  $\text{KMnO}_4\text{-H}_2\text{SO}_4$ ) modes. The characteristic XRD peak of pGFW at  $2\theta=26.45\text{--}26.50^\circ$  completely disappears during the oxidation process (Fig.3) due to complete oxidation of pGFW into graphene oxide. XRD analysis also confirmed that both oxidation methods led to the GO-phases characterized with the peaks located at  $2\theta = 10.90$  and  $10.60^\circ$ , respectively (Fig. 3). The obtained results correspond to the available data of processes used flake graphite or expanded graphite as a precursor.<sup>4,13,14</sup> In case of low-temperature mode oxidation of pGFW, the C/O ratio (at.%) was found to be 61:38. During its reduction with ascorbic acid, the C/O ratio was modified to be 81:19. The peak of GO at  $2\theta = 10.90^\circ$  completely disappeared during the reduction process and appeared a broad diffraction maximum for rGO at  $2\theta=23.80^\circ$ .

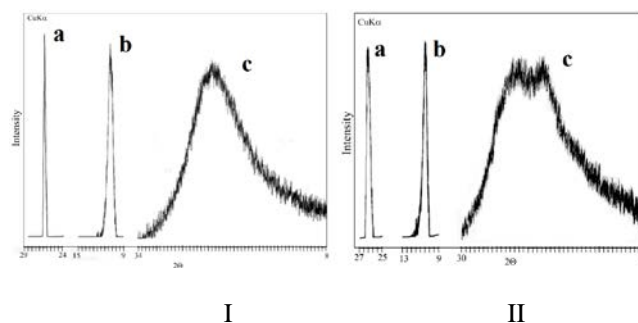


**Figure 3.** XRD patterns of graphite foil (Ia), GO (Ib), rGO (Ic), and pGFW (IIa), GO (IIb), rGO (IIc). GO was obtained by oxidation of pGFW with  $\text{KMnO}_4\text{-NaNO}_3\text{-H}_2\text{SO}_4$  (Ib) and with  $\text{KMnO}_4\text{-H}_2\text{SO}_4$  (IIb).

When the pGFW was oxidized in a high temperature mode ( $\sim 50^\circ\text{C}$ ,  $\text{KMnO}_4\text{-H}_2\text{SO}_4$ ), the C/O ratio (at.%) was found to be 64:35. In case of its reduction with ascorbic acid, rGO is obtained and the C/O ratio (at.%) was changed to 80:20. The diffraction peak at  $2\theta = 10.6^\circ$  disappeared and two peaks of rGO appeared at  $2\theta = 21.2$  and  $23.7^\circ$  (the sample was dried in vacuum at  $150^\circ\text{C}$  in 2 h).

During the reduction of GO to rGO by the different methods, the diffraction peak maximums appeared at different values of  $2\theta$  between  $20.0$  and  $26.6^\circ$ .<sup>4,13,14</sup> The location of the peaks depended on the rGO drying temperature and shifted to higher values with increasing that. Using the hydroiodic acid solution (57 %) to reduce GO obtained by us, this diffraction maximum could be detected at  $2\theta=23.7^\circ$ . Natural flake graphite pGFW oxidation required 8–15 % more sulfuric acid because the viscosity of the reaction medium, but it confirmed that the powder oxidation process effectively passed using 93–95 % sulfuric acid as well because it is cheaper and easier available than the concentrated  $\text{H}_2\text{SO}_4$  (98 %).

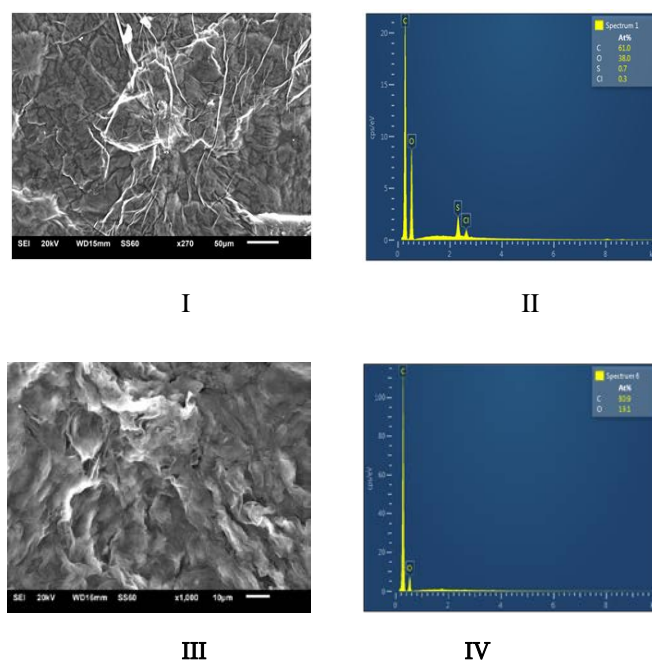


**Figure 4.** SEM image (I and III) and EDX spectrum (II and IV) of GO platelets and rGO sheets, respectively.

The method of synthesis of GO and its separation from the reaction mixture was partially corrected in a way that the experiments would finish after 8–10 h only. Sulfuric acid and metal ions ( $K^+$ ,  $Na^+$ , and  $Mn^{2+}$ ) were removed with decanting (2 times with  $H_2O$ , 3 times with 5% HCl solution). A 5 % solution of HCl precipitates GO-flakes in 7–10 min, thus, the process to remove the main impurities could be accelerated. Subsequent GO purification was carried out using traditional centrifuging and washing methods.

It is confirmed that the received GO (Figure 4) contains sulfur and chlorine as impurities, S:Cl atomic ratio (at.%) was found to be 0.7:0.3. A similar result was obtained using flake graphite (0.7–2.8):(0.6–0.8).<sup>8,9</sup> These impurities can be removed during the reduction process of GO. The decanted solutions contained 12–17 wt.% GO, but the large volume of the solutions complicated the separation.

It is easier to remove the GO from these acidic solutions in its reduced form. In strong acidic solutions, GO can be reduced to rGO using various chemical reagents.<sup>12,13</sup> We selected ascorbic acid to reduce GO in solutions to rGO (Figure 4) at 80°C. The EDX analysis confirmed the completeness of reduction and elimination of the chlorine and sulfur-containing contaminants. □

Using a high-temperature (1000–1500°C) thermal treatment, the reduced graphene oxide can be transformed into graphene with a defect structure.

## Conclusions

Grinding of waste industrial graphite foils resulted in graphite powders (pGFW) with a particle size of <140  $\mu m$ , which oxidation to obtain GO was carried out with  $KMnO_4$ – $NaNO_3$ – $H_2SO_4$  oxidation system (Hummer method). The C/O ratio in GO and its ascorbic acid reduced form (rGO) were found to be 61:38 and 81:19, respectively. It was confirmed that GO could also be obtained from pGFW using  $KMnO_4$ – $H_2SO_4$  system as well at 50 °C. Industrial wastes of graphite foils were found to be appropriate precursors for an eco-friendly synthesis of GO and rGO, which can be transformed into graphene by thermal treatment at high temperature.

## Acknowledgments

We would like to thank Dr. Vakhtang Ugrekhelidze (National High Technology Center, Tbilisi, Georgia), who provided us with graphite foil samples.

Paper was presented at the 5th International Conference “Nanotechnologies”, November 19–22, 2018, Tbilisi, Georgia (Nano–2018).

## References

- <sup>1</sup>Panatarani C., Muthahhari N., Rianto A., Joni I. M., Purification and preparation of graphite oxide from natural graphite, *AIP Conf. Proc.*, **2016**, 1719, 030022, 6 pp, <https://doi.org/10.1063/1.4943717>
- <sup>2</sup>Ambrosi A., Chua Ch. K., Khezri B., Sofer Z., Webster R. D., Pumera M., Chemically reduced graphene contains inherent metallic impurities present in parent natural and synthetic graphite, *Proc. Natl. Acad. Sci. USA*, **2012**, 109(32), 12899–12904. <https://doi.org/10.1073/pnas.1205388109>
- <sup>3</sup>Dimiev A. M., Eigler S., Eds. *Graphene Oxide: Fundamentals and Applications*, Chichester, Wiley, **2016**, 432 pp.
- <sup>4</sup>Hu X., Yu Y., Zhou J., Song, L., Effect of graphite precursor on oxidation degree, hydrophilicity and microstructure of graphene oxide, *Nano: Brief Rep. Rev.*, **2014**, 9(3), 1450037, 8 pp. DOI: 10.1142/S1793292014500374
- <sup>5</sup>Kaniyoor A., Baby T. T., Ramaprabhu S., Graphene synthesis via hydrogen induced low-temperature exfoliation of graphite oxide, *J. Mater. Chem.*, **2010**, 20, 8467–8469. DOI: 10.1039/C0JM01876G
- <sup>6</sup>Chen T., Zeng B., Liu J. L., Dong J. H., Liu X. Q., Wu Z., Yang X. Z., Li Z. M., High throughput exfoliation of graphene oxide from expanded graphite with the assistance of strong oxidant in modified Hummers method, *J. Phys. Conf. Ser.*, **2009**, 188, 012051, 5 pages, <https://doi.org/10.1088/1742-6596/188/1/012051>
- <sup>7</sup>Pakhira B., Ghosh S., Maity S., Sangeeth, D. N., Laha A., Allam A., Sarkar S., Extraction of preformed graphene oxide from coal: its clenched fist form entrapping large molecules, *RSC Adv.*, **2015**, 5(108), 89076–89082. DOI: 10.1039/C5RA15699H
- <sup>8</sup>Marcano D. G., Kosynkin D. V., Berlin J. M., Sinitskii A., Sun Zh., Slesarev A., Alemany L. B., Lu W., Tour J., *ACS Nano*, 2010, 4(8), 4806–4814.
- <sup>9</sup>del Prado Lavin Lopez M., Valverde Palomino J. L., Sanchez Silva M. L., Romero Izquierdo A.. In: *Recent Advances in Graphene Research*, 2016, INTECH, 122–133. <http://dx.doi.org/10.5772/63752>
- <sup>10</sup>Sun L., Fugetsu B., Mass production of graphene oxide from expanded graphite, *Mater. Lett.*, **2013**, 109, 207–210. <https://doi.org/10.1016/J.MATLET.2013.07.072>,
- <sup>11</sup>Yang H., Li H., Zhai J. Sun L., Yu H., Simple Synthesis of Graphene Oxide Using Ultrasonic Cleaner from Expanded Graphite, *Ind. Eng. Chem. Res.*, **2014**, 53(46), 17878–17883. DOI: 10.1021/ie503586v
- <sup>12</sup>Gambhir S., Jalili R., Officer D. L., Wallace G. G. Chemically converted graphene: scalable chemistries to enable processing and fabrication, *NPG Asia Mater.*, **2015**, 7, e186, 15 pp. <https://doi.org/10.1038/am.2015.47>
- <sup>13</sup>Aunkor M. T. H., Mahbulul I. M., Saidur R., Metselaar H. S. C., The green reduction of graphene oxide, *RSC Adv.*, **2016**, 6, 27807–27828. DOI: 10.1039/C6RA03189G
- <sup>14</sup>Muzyka R., Kwoka M., Smedowski L., Diez N., Gryglewicz G., Characterization of Graphite Oxide and Reduced Graphene Oxide Obtained from Different Graphite Precursors and Oxidized by Different Methods Using Raman Spectroscopy, *New Carbon Mater.*, **2017**, 32(1), 15–20. doi: 10.3390/ma11071050

- <sup>15</sup>Botas C., Perez-Mas A. M., Alvarez P., Santamaria R., Granda M., Blanco C., Menedez R., Optimization of the size and yield of graphene oxide sheets in the exfoliation step, *Carbon*, **2013**, *63*, 562-592.  
<http://dx.doi.org/10.1016/j.carbon.2013.06.096>
- <sup>16</sup>Alam S. N., Sharma N., Kumar L., Synthesis of Graphene Oxide (GO) by Modified Hummers Method and Its Thermal Reduction to Obtain Reduced Graphene Oxide (rGO), *Graphene*, **2017**, *6(1)*, 1-18. DOI: [10.4236/graphene.2017.61001](https://doi.org/10.4236/graphene.2017.61001)
- <sup>17</sup><http://www.toyotanso.com/Products/perma-foil/>
- <sup>18</sup>Rem W., Cheng H. M., The global growth of graphene, *Nature Nanotechnol.*, **2014**, *9*, 726-730

Received: 06.01.2018  
Accepted: 26.02.2019.